BBA - Biomembranes 1864 (2022) 183872

Contents lists available at ScienceDirect

BBA - Biomembranes

journal homepage: www.elsevier.com/locate/bbamem

Mycobacterium abscessus cell wall and plasma membrane characterization by EPR spectroscopy and effects of amphotericin B, miltefosine and nerolidol

Lais Alonso [a,*], Laryssa Ketelyn Lima Pimenta [b], André Kipnis [b], Antonio Alonso [a,*]

[a] Instituto de Física, Universidade Federal de Goiás, Goiânia, GO, Brazil
[b] Instituto de Patologia Tropical e Saúde Publica, Departamento de Biociências e Tecnologia, Universidade Federal de Goiás, Goiânia, GO, Brazil

ARTICLE INFO

Keywords:
Mycobacterium abscessus
Amphotericin B
Miltefosine
Nerolidol
Spin label
Electron paramagnetic resonance

ABSTRACT

Spin label electron paramagnetic resonance (EPR) spectroscopy was used to characterize the components of the *Mycobacterium abscessus massiliense* cell envelope and their interactions with amphotericin B (AmB), miltefosine (MIL), and nerolidol (NER). Spin labels analogous to stearic acid and phosphatidylcholine (PC) were distributed on an envelope layer with fluidity comparable to other biological membranes, probably the mycobacterial cell wall, because after treatment with AmB a highly rigid spectral component was evident in the EPR spectra. Methyl stearate analogue spin labels found a much more fluid membrane and did not detect the presence of AmB, except for at very high drug concentrations. Unlike other spin-labeled PCs, the TEMPO-PC spin probe, with the nitroxide moiety attached to the choline of the PC headgroup, also did not detect the presence of AmB. On the other hand, the steroid spin labels were not distributed across the membranes of *M. abscessus* and, instead, were concentrated in some other location of the cell envelope. Both MIL and NER compounds at 10 μM caused increased fluidity in the cell wall and plasma membrane. Furthermore, NER was shown to have a remarkable ability to extract lipids from the mycobacterial cell wall. The EPR results suggest that the resistance of mycobacteria to the action of AmB must be related to the fact that this drug does not reach the bacterial plasma membrane.

1. Introduction

Mycobacteria are known to have a cell wall that is abundantly composed of mycolic acids as well as a plasma membrane, which together form a structure known as the cell envelope [1,2] that makes the species of this genus intrinsically resistant to many antimicrobials [3]. Additionally, the list of antimicrobials that are active against infections caused by mycobacteria species is limited, and this is further reduced by their specific activity against only certain complexes to which the species belong. For instance, the *Mycobacterium tuberculosis* complex bacteria, responsible for the high rate of tuberculosis cases around the world, are responsive to the first class group of antimicrobials such as rifampin, isoniazid, ethambutol, and pyrazinamide. Conversely, the most indicated drugs for the treatment of *M. abscessus* complex bacteria, a group of opportunistic pathogens causing hospital-acquired infection outbreaks, are the macrolides (clarithromycin and amikacin) and cefoxitin [4], as these bacteria are known to be resistant to antituberculosis drugs [5]. To make the matter worse, mycobacteria can develop resistance to the drugs used, which poses a greater risk to public health by further reducing the effective treatments against these infectious diseases [3]. Thus, the prospection and discovery of new drugs with action against this exclusive group of bacteria is of uttermost importance.

Electron paramagnetic resonance (EPR) spectroscopy associated with the spin label method has previously been used to study the mechanisms of antileishmanial activity of the membrane-active compounds, amphotericin B (AmB), miltefosine (MIL), and nerolidol (NER) [6–13]. All three compounds were shown to cause remarkable changes in plasma membrane fluidity at concentrations associated with their antileishmanial activities [6–13]. However, the modes of action of these compounds are still unclear. For instance, in the case of AmB, which is also used an antifungal drug, the most widely accepted and studied mechanism of action is the one proposed by the ion channel model, in which AmB-sterol complexes form transmembrane channels permeable to ions that lead to cell death [14,15]. However, the fact that the channel-forming capacity of AmB is not always required for fungicidal

* Corresponding author.
E-mail address: alonso2233@gmail.com (L. Alonso).

https://doi.org/10.1016/j.bbamem.2022.183872
Received 12 October 2021; Received in revised form 24 December 2021; Accepted 19 January 2022
Available online 24 January 2022

action gave rise to the sterol sponge model, in which AmB would form large extramembranous aggregates that extract the sterol from lipid bilayers [14]. Recent studies by EPR have shown that AmB does not actually enter the lipid bilayer but the EPR spectra were consistent with the rapid entry of AmB into cell membranes [6,7], indicating a role for membrane proteins in the process of AmB entry. Furthermore, the flip-flop movement between the two membrane leaflets is not known and could also be protein-dependent [6].

MIL is a synthetic phospholipid analogue (hexadecylphosphocholine), which has demonstrated activity against several *Leishmania* species [16], a broad spectrum of pathogenic fungi [17,18], various strains of *Acanthamoeba* [19], *Streptococcus pneumoniae* [20], *Staphylococcus aureus* [21], and *Schistosoma mansoni* [22]. NER is an acyclic sesquiterpene with an abundant presence in essential plant oils, which has already been approved by regulatory agencies, including the FDA, for food use. It has been reported that NER exhibits *in vitro* activity against *M. abscessus* [23] and several other bacteria [24], fungi [25,26], and the parasites, *Trypanosoma* [27], *Leishmania* [28], *Plasmodium* [29], and *Babesia* [30]. Therefore, considering the broad spectrum of activity of the MIL and NER compounds, the mechanisms of action based on cell membrane attack seem consistent.

In this work we use EPR spectroscopy to study the interactions of various spin labels with the cell wall and plasma membrane of *M. abscessus*. As the interactions of AmB, MIL, and NER with membranes of the *Leishmania* parasite, erythrocyte, and macrophage have already been extensively studied using the EPR technique [6–13], we decided to examine their interactions with the *M. abscessus* cell envelope in order to obtain additional information. Although the mycobacterial cell envelope does not contain sterol, AmB showed interactions with membrane spin labels. However, it was interpreted that AmB only affects the cell wall and essentially does not reach the mycobacterial plasma membrane, which could explain the lack of antibacterial activity of this compound against this species. On the other hand, MIL and NER affected both the cell wall and the plasma membrane of the mycobacteria.

2. Materials and methods

2.1. Chemicals

The spin labels, 5- and 16-DOXYL stearic acid (5- and 16-DSA), methyl 5- and 16-doxyl-stearate (5- and 16-DMSA), 3-DOXYL-17β-hydroxy-5α-androstane (androstane), and 3β-DOXYL-5α-cholestane (cholestane) (Fig. 1), as well as amphotericin B (AmB; A9528, a colloidal suspension containing ~45% AmB, 35% sodium deoxycholate, sodium phosphate, and sodium chloride) and nerolidol (NER; 98% purity, a mixture of cis and trans nerolidol, MW = 222.37 g/mol, CAS Number 7212-44-4) were purchased from Sigma-Aldrich (St. Louis, MO, USA). The spin labels, 1-palmitoyl-2-stearoyl-(5- and 16-DOXYL)-sn-glycero-3-phosphocholine (5- and 16-PC) and 1,2-dipalmitoyl-sn-glycero-3-phospho(tempo) choline (TEMPO-PC) (Fig. 1), as well as miltefosine (MIL) were purchased from Avanti Polar Lipids Inc. (Alabaster, AL, USA).

2.2. Bacterial strain and minimum inhibitory concentration (MIC) test

To analyze whether AmB, MIL, and NER had an inhibitory effect on mycobacteria, *M. abscessus* subsp. *massiliense* isolate GO-06, a reference

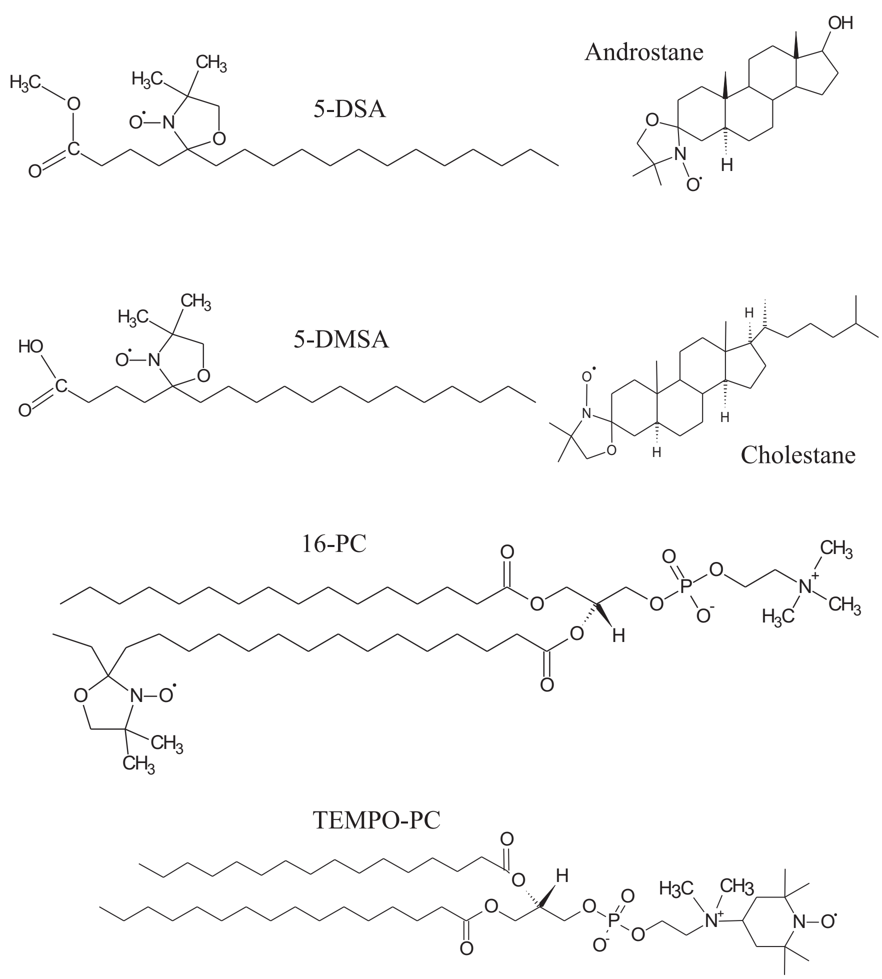

Fig. 1. Structures of spin labels used in this work.

strain isolated from an outbreak that occurred in Goiânia, State of Goiás, Brazil during 2005 and 2007 [31], was used. The strain, maintained in our bacterial collection (Brazilian Culture Collection of the Institute of Tropical Pathology and Public Health BCCIPTSP – WDCM #1223), was grown in Mueller Hinton broth (MH; HiMedia, Mumbai, India) with 0.05% Tween 80 at 35 °C with agitation (200 rpm) for three days. The culture concentration was adjusted to a 0.5 McFarland standard (approximately 1.5×10^8 CFU/mL) after vigorous homogenization to dissolve clumps.

The MIC was determined according to ATS/IDSA recommendations [32]. Bacterial cultures were further adjusted so that 200 CFU were deposited into each well of a 96-well microplate that contained serially diluted drugs (MIL and NER) in levels ranging from 20 to 0.078 mM. Different concentrations of ethanol (used as diluent for the compounds) and amikacin (1 μg/mL) were included as controls. The plates were incubated for three days at 35 °C, after which serial dilutions of each well were plated on MH agar to determine the mycobacteria concentration. The MIC was determined as the lowest concentration without bacterial growth. Alternatively, the percentage of growth inhibition was determined by comparing the number of CFU obtained in a specific condition compared to the CFU obtained with the growth control plate without any drug.

2.3. Membrane spin labeling and treatment of the cells

M. abscessus cells were washed three times in PBS (prepared with ultrapure water) by centrifugation at 25,000 ×*g* for 10 min at 4 °C. The bacterial concentration was then adjusted to 1.2×10^{10} CFU/mL. For the EPR experiments, 50 μL of this cell suspension was then diluted in PBS to either 2 mL (3×10^8 CFU/mL) or 10 mL (6×10^7 CFU/mL). AmB was diluted in PBS to 9 mM, while MIL and NER were diluted in ethanol to 50 mM. The 2 or 10 mL bacterial suspensions were then treated with different concentrations of AmB, MIL, and NER and incubated for 90 min at room temperature in the dark. After this period, the samples were centrifuged at 25,000 ×*g* for 10 min at 4 °C, the supernatant was discarded leaving a volume of 50 μL that contained the cell pellet. The samples were agitated for homogenization and spin-labeled. The spin labels were dissolved in ethanol (5 mg/mL) and, using a microsyringe of 5 μL, a 0.2 μL aliquot was added to each sample. Each sample was transferred to a 1-mm-i.d. capillary tube, which was flame-sealed, and centrifuged at 25,000 ×*g* for 5 min at 20 °C. The cell pellet formed gave an estimated volume of 5.5 μL for the control samples (untreated cells). Then the EPR measurements were taken.

The EPR spectra were recorded using an EMX-Plus spectrometer from Bruker (Rheinstetten, Germany), operating in the following instrumental settings: microwave power, 20 mW (this is a considered high power that could cause power saturation behavior of the EPR signal or some heating of the samples. However, we found that the changes in the spectra line shape were imperceptible, and the higher power provided an advantage by considerably improving the signal-to-noise ratio); microwave frequency, 9.452 GHz; modulation frequency, 100 kHz; modulation amplitude, 1.0 G; magnetic field scan, 100 G; sweep time, 168 s; and sample temperature, 25 °C.

Best-fit EPR spectra were obtained using the nonlinear least-squares (NLLS) software developed by Freed JH and coworkers [33,34]. The rate of rotational Brownian diffusion, R_{bar}, provided by the NLLS fitting program was converted to the parameter of rotational correlation time, τ_c, using the relationship $\tau_c = 1/6R_{bar}$ [34]. EPR spectra were simulated using a model of one or two spectral components with the same input parameters for magnetic tensors g and A: $g_{xx} = 2.0082$; $g_{yy} = 2.0058$; $g_{zz} = 2.0025$; $A_{xx} = 6.0$ G; $A_{yy} = 6.3$ G; $A_{zz} = 31.4$ G.

2.4. Statistical analysis

Data expressed as mean and standard deviation were obtained from at least three independent experiments. Using the OriginPro 8.5 program, the means were compared through a one-way analysis of variance (ANOVA). Tukey's test was used to identify significant differences ($P < 0.05$) between means among the different treatments.

3. Results and discussion

3.1. Activity of MIL, NER, and AmB against M. abscessus

The antibacterial activity of NER was evaluated against *M. abscessus* subsp. *massiliense* GO-06 isolate resulting in an MIC of 10 mM, while a concentration of 1.25 mM was able to inhibit 90.5% of the mycobacteria growth and there was 78.5% of inhibition at 0.15 mM. NER presented an MIC ten times smaller than that shown previously by Pereira et al. [23]; whether this difference is due to the laboratory techniques of the *M. abscessus* strains used has not yet been evaluated. MIL, in turn, presented an MIC of 5 mM, with 90.5% inhibition at 0.625 mM and 38.5% inhibition at 0.078 mM. This is the first report to our knowledge of the bactericidal activity of MIL against a *Mycobacterium* species. AmB did not present inhibitory activity at any of the concentrations tested. Ethanol, which was used as diluent for the compounds, did not inhibit mycobacteria growth at the concentrations corresponding to where an MIC was detected for the analyzed drugs.

3.2. Lipid dynamics in cell wall and plasma membrane of M. abscessus subsp. massiliense

Fig. 2A shows the EPR spectra of the lipid spin label 5-DSA (Fig. 1) incorporated in the lipid domain of *M. abscessus* for untreated and AmB-treated samples. The EPR parameter $2A_{//}$ (outer hyperfine splitting), associated with probe mobility, showed a value of 54.1 G for untreated *M. abscessus* membranes, indicating that they are more fluid than that which has been reported for *L. amazonensis* ($2A_{//}$ of ~56 G) and erythrocytes ($2A_{//}$ of ~57 G) [8–13]. In the cell membrane, the spin label 5-DSA behaves like an annular or boundary lipid that contacts the hydrophobic surfaces of membrane proteins. For membranes with low protein content, the EPR spectrum shows the spectral resolution between the spin probes motionally restricted by direct contact with the proteins and those located in the bilayer bulk phase [35,36]. However, for membranes with a large content of proteins, as is the case of the erythrocyte or *Leishmania* (around 50% of membrane volume), only the spectral component corresponding to the spin label contacting protein appears in the EPR spectra of 5-DSA. Thus, the mobility of this lipid probe can also be strongly influenced by the dynamics of the membrane protein component. This greater membrane fluidity of *M. abscessus* compared to that of erythrocytes and *Leishmania* may perhaps be explained by a lower protein content or lack of sterols.

With the addition of AmB, the EPR spectra were characterized by the coexistence of two spectral components of very distinct mobility states. These components can be assigned to two populations of spin labels: those that do and those that do not come in contact with the hydrophobic surface of the AmB molecule. As indicated in Fig. 2A, the least motional affected component has a $2A_{//}$ parameter value similar to the control (~54 G, separation indicated by the two black dotted lines), while the restricted motional component has a $2A_{//}$ value of ~61.5 G (separation indicated by two red dotted lines). The increase in AmB concentration in the *M. abscessus* sample increases the population of AmB-affected spin probes, as deduced by the increase in resonance line intensities at the positions indicated by the red dotted lines. Interestingly, these EPR spectra also show the three resonance lines (indicated by arrows) of a small fraction of probe free in the aqueous phase. This fraction of free probes decreases with increasing AmB concentration, indicating that this spin probe undergoes a membrane/water partition in the mycobacterium suspension, and that the addition of AmB, increasing the membrane volume, leads to an increase in the amount of probe inserted into the membrane.

On the other hand, when *M. abscessus* membranes were spin-labeled

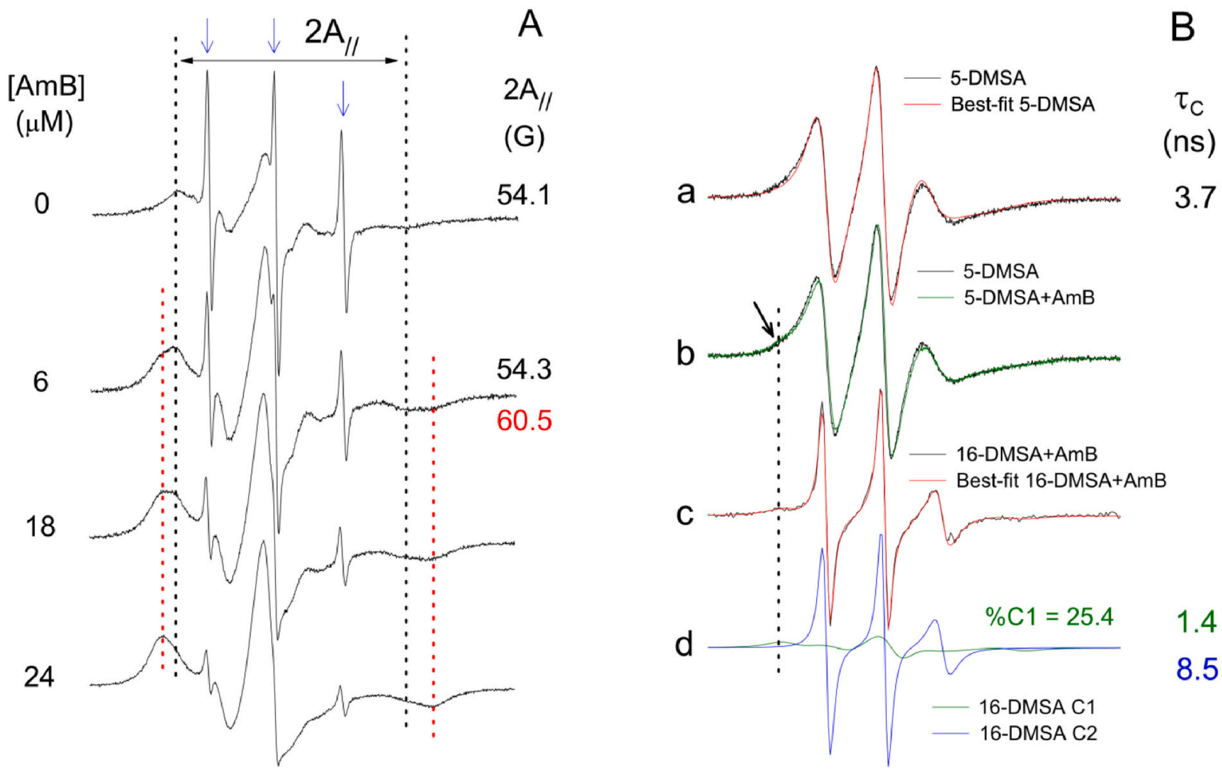

Fig. 2. EPR spectra of different spin probes incorporated in *Mycobacterium abscessus* membranes for untreated (control) and AmB-treated samples. (A) Spin label 5-DSA (Fig. 1) and treatment with different concentrations of AmB. The values of the parameter $2A_{//}$ (external hyperfine splitting, given by the separation in magnetic field units between the external resonance lines) are indicated for various spectra. With the addition of AmB a motional restricted spectral component appears in the EPR spectrum, with a $2A_{//}$ value of ~60.5 G (indicated by the two red lines). The arrows indicate three resonance lines from a small fraction of spin label freely tumbling in the aqueous phase (outside the membranes). (B) (a) Experimental (black line) and best-fit (red line) EPR spectra of 5-DMSA (Fig. 1) in untreated *M. abscessus*; the rotational correlation time, τ_C, value is indicated. (B) (b) Experimental spectra of 5-DMSA for untreated *M. abscessus* (black line) and treated with 50 μM AmB (green line); the arrow indicates a very small change in the spectrum that could be caused by the presence of AmB. (B) (c) Experimental (black line) and best-fit spectra (red line) of 16-DMSA in *M. abscessus* treated with 50 μM AmB; the spectrum shows an additional restricted motional component of a fraction of probes that interact with AmB, which is noted by the peak at the magnetic field position indicated by the vertical dotted line. (B) (d) Spectral components that make up the simulated spectrum shown in (c); in green the component of spin probes that interact with AmB (25.4%) is shown, and in blue, the component of probes without this interaction (75.6%). The total scan range of the magnetic field for each spectrum was of 100 G (X axis), and the intensity is in arbitrary units (Y axis). (For interpretation of the references to color in this figure legend, the reader is referred to the web version of this article.)

with 5-DMSA, which differs from 5-DSA solely by replacing the hydrogen of the carboxyl group with methyl, a very fluid membrane was observed (Fig. 2B). Furthermore, this spin label did not detect any change in the membrane fluidity following treatment with AmB, except at very high drug concentrations. For treatment with 50 μM AmB, a small fraction of a lower mobility component appeared due to probe interactions with the AmB molecule (Fig. 2B (b)). These results suggest that 5-DSA is incorporated in the cell wall and 5-DMSA in the plasma membrane, and that AmB inserts into the cell wall of *M. abscessus* subsp. *massiliense* almost completely.

In our experiments, EPR spectra were recorded approximately 15 min after membrane spin labeling. It is important to mention that there was a loss of EPR signal due to the reduction of the spin label nitroxide, which occurs mainly by reaction with thiol groups. We noticed that within 15 min there was a signal loss of approximately 20%. For a relatively short time after spin labeling, the spin labels would be expected to be predominantly embedded in the cell wall. However, it may be possible that 5-DMSA has some way of accessing the plasma membrane more quickly. To examine whether AmB could interact with 5-DMSA if it had access to the cytoplasmic side of the envelope, we caused a partial lysis of the cells. For this, 2 mL of ultrapure water was added to 50 μL of the cell suspension in PBS (3×10^8 CFU/mL) and after 30 min the AmB was added for 30 min. To collect the maximum membrane content of the sample a centrifugation was done at 25,000 ×g. The 5- and 16-DMSA spin labels now inserted into these mycobacterial membranes showed interactions with AmB (Fig. 3). However, the intensities of the EPR spectra were quite low due to the reduction of the nitroxide radical of the probes by exposure to the cytoplasmic content. The lysis procedure used did not significantly alter the control EPR spectra (untreated samples) of probes 5- and 16-DMSA (Figs. 2B and 3). These results suggest that when the cytoplasmic side of the envelope is exposed to AmB it interacts with the 5- and 16-DMSA probes that are likely inserted into the plasma membrane. Based on previous work [1,2], we have assembled a schematic illustration of the mycobacterial cell wall and plasma membrane, where the possible locations of the spin labels 5-DSA and 5-DMSA are indicated (Fig. 4).

Fig. 5A shows the EPR spectra of spin labels derived from the steroids androstane and cholestane, and from phosphatidylcholine, 5-PC, 16-PC, and TEMPO-PC, in *M. abscessus* subsp. *massiliense*. For the steroid spin labels, the spectra indicated strong dipolar interactions showing that the distribution of these probes in the bacterial membranes does not occur. The dipole interaction appears in the spectrum when the probes are close to each other and in the spin label method it is largely avoided by using a molar ratio between probe and membrane lipids less than 1:100. Thus, the spectra of cholestane and androstane are consistent with the accumulation of probes somewhere in the bacterial envelope. It is surprising that these steroid spin labels, which are so easily distributed in lipid bilayers and in membranes of *Leishmania*, erythrocyte, macrophage, and stratum corneum [6,37,38], find resistance in the case of mycobacteria.

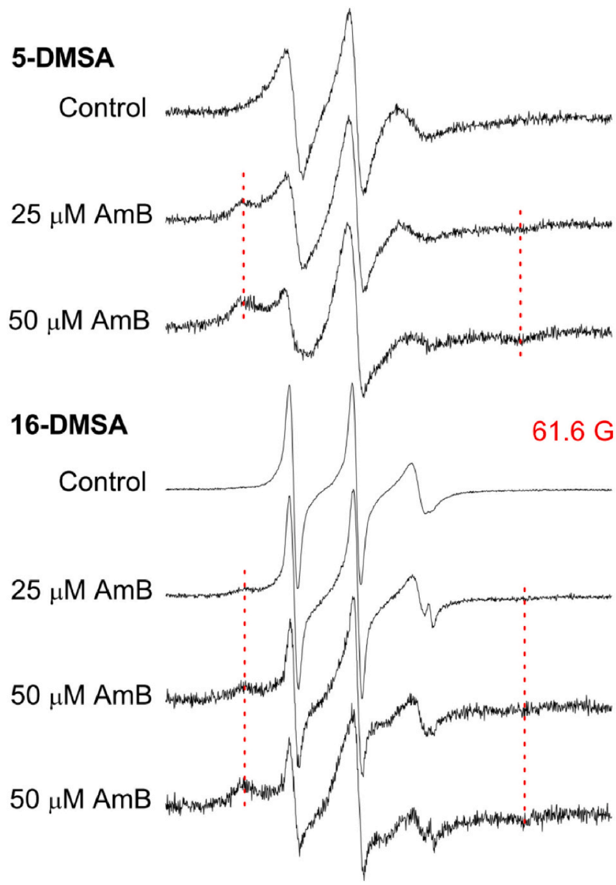

Fig. 3. EPR spectra of 5- and 16-DMSA incorporated in *Mycobacterium abscessus* membranes after partial cell lysis for untreated (control) and AmB-treated samples. The vertical lines in red indicate the low and high magnetic field positions where the motional restricted spectral component's resonance lines appear due to the interactions of the spin probe with AmB. The value of the measured 2A// parameter was 61.6 G. (For interpretation of the references to color in this figure legend, the reader is referred to the web version of this article.)

It is important to mention that the 5- and 16-PC probes in general do not enter or do not satisfactorily distribute in biological membranes. For example, we have not been able to obtain good EPR spectra of these probes in erythrocyte or *Leishmania* membranes. However, in *M. abscessus* the EPR spectra of 5- and 16-PC were relatively good and showed that these probes interact with AmB similar to 5-DSA. On the other hand, TEMPO-PC, which has a nitroxide moiety attached off the choline of the PC headgroup (Fig. 1), did not detect the presence of AmB. This result suggests that AmB enters the lipid bilayer of the cell wall rather than staying outside on the membrane surface, as predicted by the sterol sponge model. Higher concentrations of AmB were required to observe its effects when a higher concentration of mycobacteria was used (3×10^8 CFU/mL). As has been shown in several works, the dependence of the activity of a hydrophobic compound on the cellular concentration used in the assay suggests that the compound's activity is related to its action on the membrane [7,9–11,13]. However, according to our interpretation discussed above, AmB would have high affinity only for the bacterial wall. As indicated by the 16-DSA spin label in Fig. 5B, for the bacterial concentration of 6×10^7 CFU/mL, which is lower and is in the range of cell concentrations commonly used for *in vitro* assays, these probes can detect the presence of AmB at concentrations of 4 μM or less. The spin label 16-DSA, having the nitroxide moiety attached to the 16th carbon atom of the acyl chain, shows a high mobility EPR spectrum (narrow resonance lines), superimposed with the spectral component of a small fraction of free probes in the solution, as in the case of 5-DSA (Fig. 2A). But when this probe interacts with AmB in the membrane it shows an additional spectral component of low mobility, where the $2A_{//}$ parameter can be measured ($2A_{//} = \sim 60.5$ G).

As the channel formation capacity of AmB is not always necessary for the fungicidal activity [14], and the results obtained by EPR spectroscopy indicate that AmB can form aggregates with several spin labels in the biological membrane [6,7], taken together, it is likely that at higher concentrations AmB could present activity associated with its ability to form aggregates with membrane lipids. These putative short-lived aggregates would have the potential to cause transient defects in the structural dynamic of membrane lipids, which in turn could result in increased membrane permeability and electrolyte leakage.

One of the difficulties in accepting the sterol sponge model lies in the fact that AmB is able to reduce *L. amazonensis* infections in murine macrophages *in vitro* [39,40]. However, the mechanisms by which AmB could reach the amastigotes that reside within a parasitophorous vacuole in the macrophages are not known [41]. According to the sterol sponge model, AmB should be located on the outside of the macrophage membrane as AmB/sterol aggregates and thus, perhaps could eliminate the parasite while also killing the macrophage. Otherwise, for AmB to gain access to the amastigotes, it would need to cross the plasma membrane of the macrophage, followed by the membrane of the parasitophorous vacuole, and then interact with the membrane of the parasite. EPR experiments have demonstrated that AmB does not actually enter lipid bilayers, but have suggested that it readily enters *Leishmania*, erythrocyte, and macrophage membranes [6,7]. And so, a role for membrane proteins in the process of AmB entry into the plasma membrane, and also in the flip-flop of the molecule, has been proposed [6].

MIL and NER caused a small increase in lipid fluidity, as indicated by the spin labels 5-DSA (which supposedly inserts into the cell wall) and 5-DMSA (which supposedly inserts into the plasma membrane) (Figs. 2 and 6). Our experiments were performed using the mycobacteria suspended in PBS and after 90 min of incubation with the compounds the samples were centrifuged and the supernatant was discarded. For higher concentrations of MIL and NER (60 μM), the presence of micelles of these compounds in the supernatant was detected (Fig. 7). Furthermore, it can be noted that the amount of membrane in the treated samples decreased, as deduced by the increase in free signal of the EPR spectra (Fig. 6A). As the spin label undergoes a membrane/water partition, a reduction in membrane volume (due to the extraction of lipids incorporated in the compound micelles, which were discarded with the supernatant), results in an increase in free signal. These experiments suggest that MIL and NER compounds at higher concentrations are able to extract lipids from the bacterial envelope through their incorporation into the compounds' micelles.

Several works using EPR spectroscopy have shown that MIL has little or no effect on lipid bilayers [42,43], but has remarkable effects on biological membrane proteins [8–13]. In contrast, NER also has strong effects on biological membranes, but acting in the lipid phase [12,13,44]. It has been proposed that NER and other sesquiterpenes/monoterpenes increase membrane lipid dynamics by acting as molecular spacers that lead to the weakening of the hydrogen bond network at the membrane polar interface [37,38,45]. It has been shown that NER can also act as extractors of a spin-labeled lipid from the lipid bilayer [46]. In our experiments we used 6×10^8 CFU/sample and as the samples were introduced in capillary it was possible to monitor the pellet volume after centrifugation, which was approximately 5.5 μL. This even allowed us to estimate the volume of *M. abscessus* as being 9.2 fL, which is approximately 10 times smaller than that of an erythrocyte. For samples with 6×10^7 CFU/mL, a volume of 10 mL PBS with 10 μM MIL or NER was used. After centrifugation at 25,000 $\times g$, which is sufficient to precipitate isolated membranes, a decrease in the final mean volume of mycobacteria was observed for samples treated with NER (−60%) and MIL (−40%) compared to untreated control samples. These results taken together suggest that the compounds NER and MIL at 10 μM are able not only to extract lipids from the mycobacteria, but also to cause their lysis.

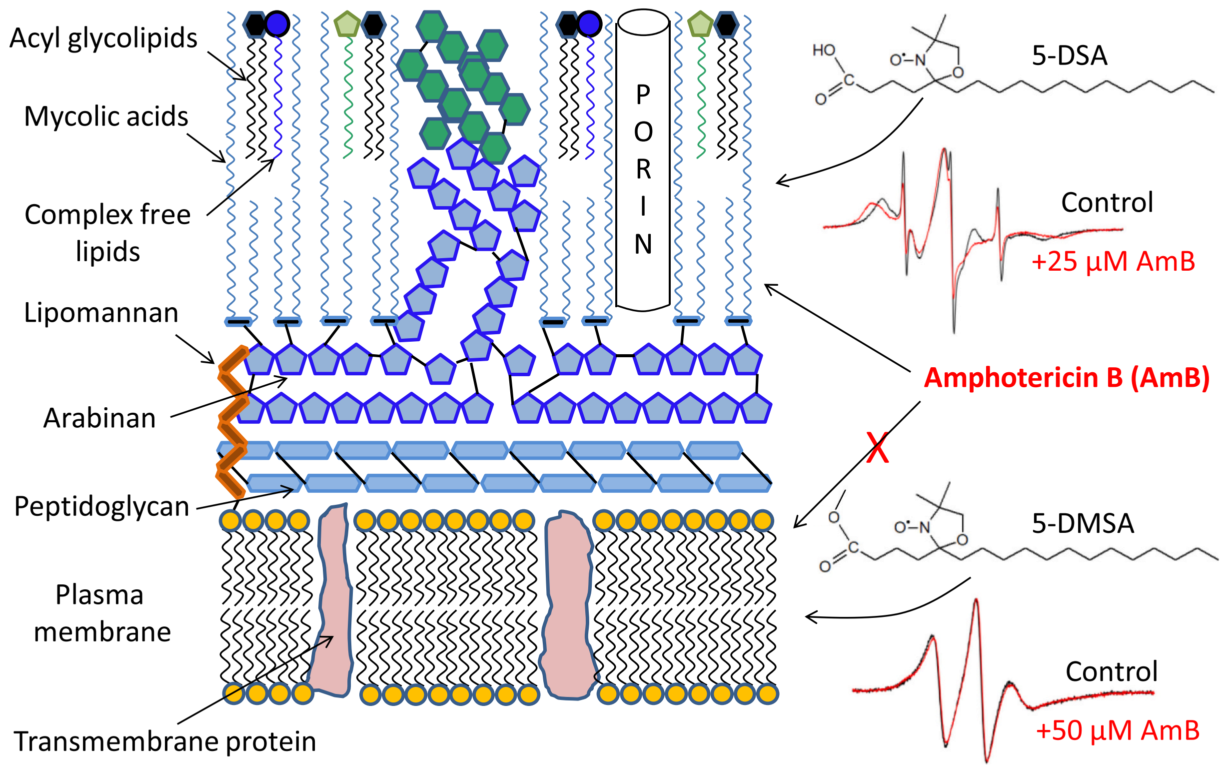

Fig. 4. Schematic representation of the mycobacterial cell wall and plasma membrane, based on figures shown in Refs. [1,2], indicating the potential location of two spin labels and AmB. It is very probable that the spin label 5-DSA is incorporated only in the cell wall, while 5-DMSA incorporates in the plasma membrane. AmB at 25 μM significantly affects the EPR spectrum of 5-DSA, but even at 50 μM it practically does not alter the spectrum of 5-DMSA.

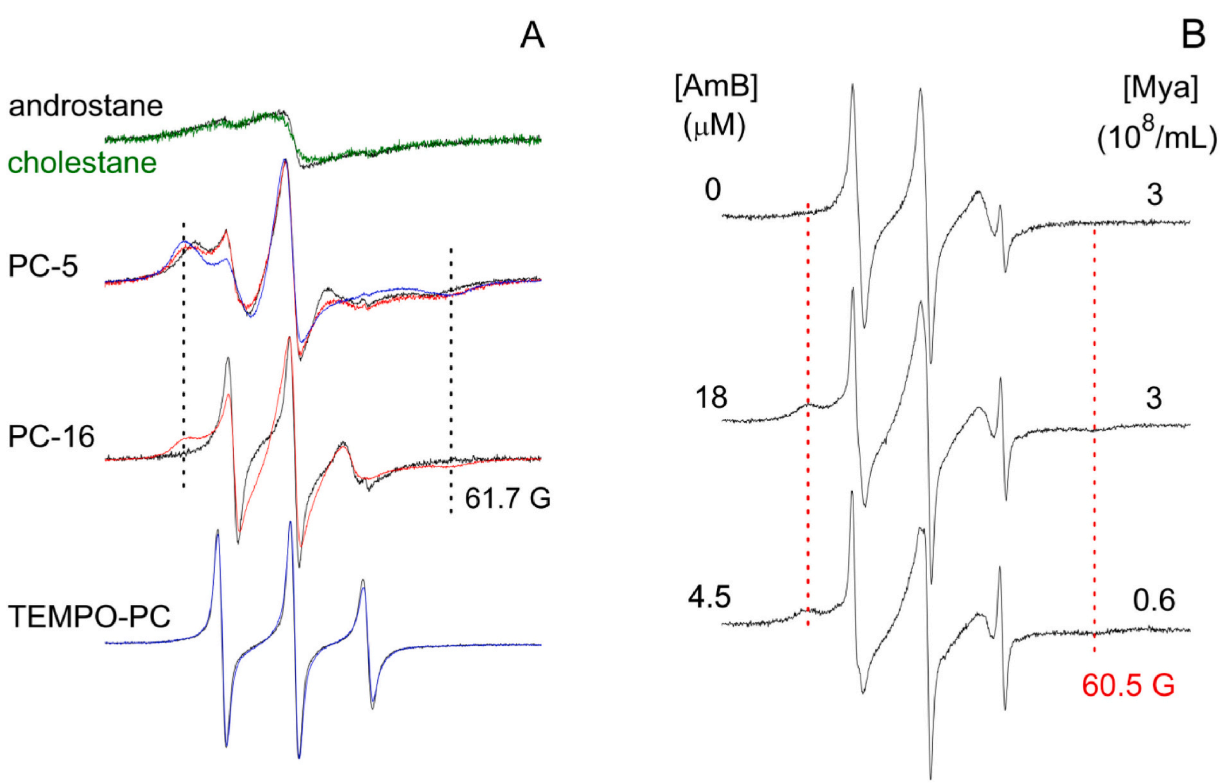

Fig. 5. (A) EPR spectra of androstane (black line), cholestane (green line), PC-5, PC-16, and TEMPO-PC in *M. abscessus* (3×10^8 CFU/mL) for untreated samples (black lines) and treated with AmB at 15 μM (red lines) and 30 μM (blue line). (B) Spin label 16-DSA for different concentrations of AmB and *M. abscessus*. (For interpretation of the references to color in this figure legend, the reader is referred to the web version of this article.)

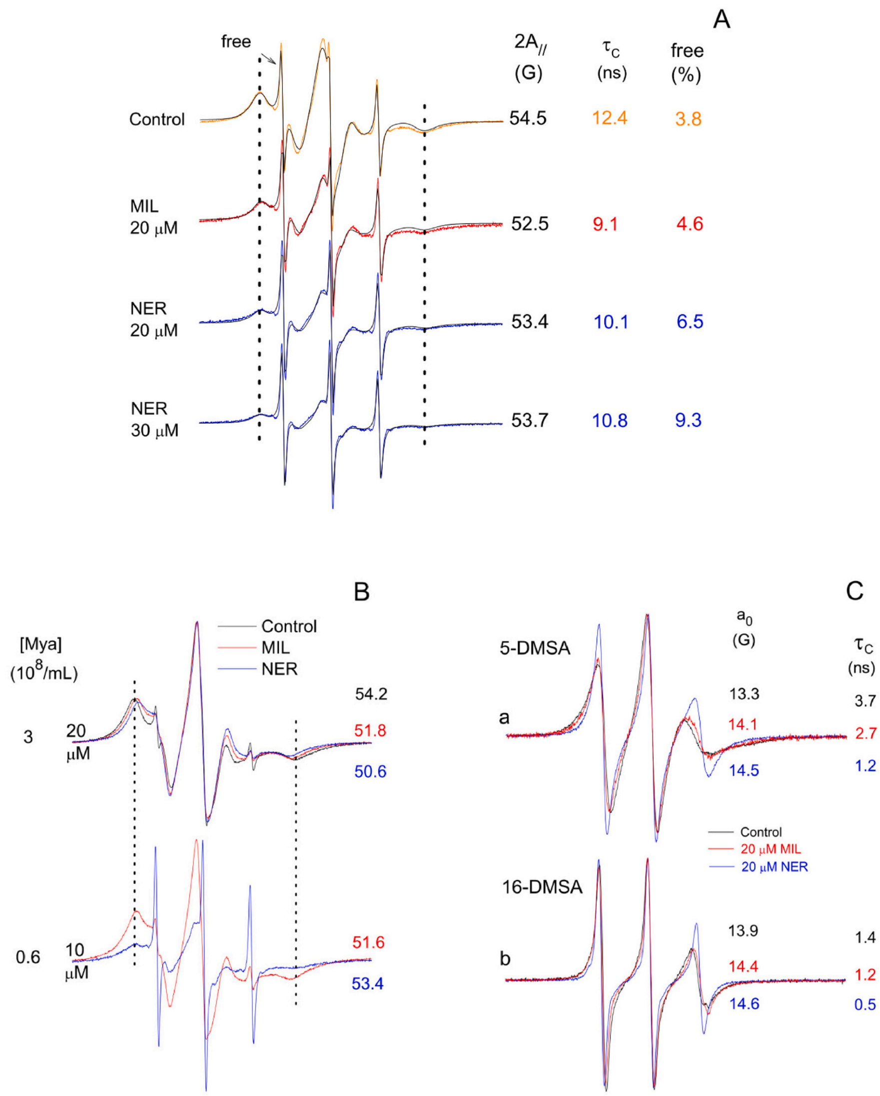

Fig. 6. EPR spectra of various spin probes embedded in *Mycobacterium abscessus* membranes: (A) 5-DSA in cell samples (3 × 10^8 CFU/mL) that were either untreated (control) or treated with 20 μM of MIL and NER. Black lines are the best-fit spectra obtained from the simulation using a two-component spectral model (spin labels in the membrane and free in solution). The τ_C and $2A_{//}$ values as well as the free component percentages are indicated. (B) EPR spectra of 5-DSA for samples with different concentrations of cells, MIL, and NER. (C) EPR spectra of 5-DMSA (a) and 16-DMSA (b) for samples of untreated control (black lines) and treated with MIL (red lines) and NER (blue lines). The ^{14}N isotropic hyperfine splitting (a_0) and τ_C values for each spectrum are indicated in the same color of respective spectra. (For interpretation of the references to color in this figure legend, the reader is referred to the web version of this article.)

The EPR signal from the mycobacterium spin-labeled with 5-DSA and treated with 10 μM NER showed an appreciable fraction of free signal, indicating that there was a large loss of lipid from the sample (Fig. 6B).

The fact that MIL and NER significantly alter the spectra of 5- and 16-DMSA indicates that these compounds also access the bacterial plasma membrane, differently to AmB. For the spectra of these spin probes that have high mobility it is not possible to measure the $2A_{//}$ parameter. Thus, we simulated the EPR spectra to obtain the τ_C parameter. For these spectra the NLLS fitting program easily finds high convergence between theoretical and experimental spectra. We do not present the simulated EPR spectra in the figure to facilitate the visualization of the experimental ones. In the EPR spectra of both spin labels represented in Fig. 6C, it can be seen that MIL increases membrane fluidity and NER increases even more, as can be seen by the reduction in τ_C values (the estimated experimental error of τ_C is 0.3 ns). Furthermore, the parameter $2a_0$, which increases with the polarity of the medium, showed that the presence of MIL increases the polarity in the membrane and that the NER increases this even more (the estimated experimental error of $2a_0$ is 0.1 G).

4. Conclusions

Spin-label EPR spectroscopy is a complementary technique that in this work, and based on the reports using these spin labels for other cells, has allowed us to generate a foundation regarding the fluidity of the *M. abscessus* membrane, the interpretations of which can be further corroborated by other techniques. The spin label derived from the stearic acid, 5-DSA, was inserted in the cell wall, where AmB showed remarkable membrane rigidity effects, while the 5-DMSA, differing only by the substitution of the carboxylic-group hydrogen by CH_3, was probably inserted in the plasma membrane, where AmB only showed small effects at concentrations 10 times higher. While the cell wall showed lipid fluidity similar to the membranes of other cells, such as that of the *Leishmania* parasite, the mycobacteria plasma membrane showed a much greater fluidity. The spin labels derived from phosphatidylcholine, 5- and 16-PC, entered the cell wall giving EPR spectra similar to those of the 5- and 16-DSA probes and were also equally sensitive to the presence of AmB. On the other hand, TEMPO-PC, in which the nitroxide moiety is on the outer surface of the membrane, did not detect the effects of AmB, suggesting that the drug enters the lipid bilayer, rather than staying adhered to the outer surface of the membrane, as predicted by the sterol sponge model. Surprisingly, the steroid spin labels androstane and cholestane showed no distribution across mycobacterial membranes, and instead concentrated somewhere in the cell envelope. The compounds MIL and NER showed increased fluidity both in the cell wall and in the plasma membrane. In the cell wall, MIL caused greater changes than NER, while in the bacterial plasma membrane the changes observed for NER were greater. MIL and NER at 10

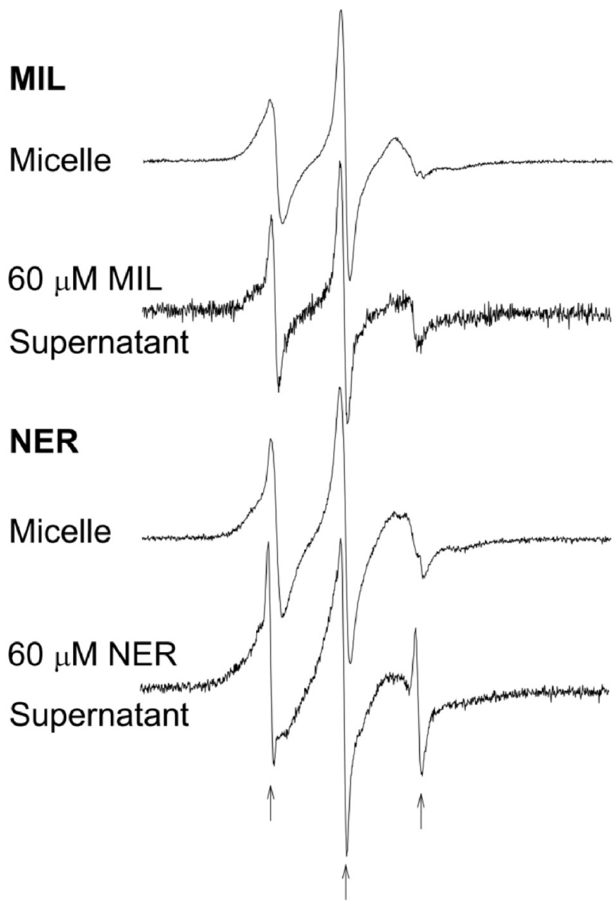

Fig. 7. EPR spectra of 5-DSA in MIL and NER micelles and in the supernatant of a cell suspension after treatment with 60 μM MIL or NER. The 5-DSA spectra indicate that the probe became incorporated into micelles present in the supernatant. The arrows indicate the positions of the three resonance lines of a fraction of free probes in the solution.

μM not only showed increases in membrane fluidity, but also lipid extraction capacity and even cell lysis. EPR results also suggested that the resistance of mycobacteria to the action of AmB is due to the fact that it does not reach the plasma membrane.

Declaration of competing interest

The authors declare that they have no known competing financial interests or personal relationships that could have appeared to influence the work reported in this paper.

Acknowledgements

This study was financially supported by grants from the Brazilian research funding agencies CNPq (445666/2014-5 and 406521/2016-6), CAPES, and FAPEG (201210267001110). Lais Alonso was a recipient of a postdoctoral fellowship from CNPq (150369/2018-2) and is currently a postdoctoral fellow at CAPES. Antonio Alonso received a research grant from CNPq (304122/2019-0). Andre Kipnis has a fellowship from CNPq (314366/2020-2).

References

[1] H. Medjahed, J.L. Gaillard, J.M. Reyrat, Mycobacterium abscessus: a new player in the mycobacterial field, Trends Microbiol. 18 (3) (2010) 117–123, https://doi.org/10.1016/j.tim.2009.12.007.
[2] R.S. Gokhale, P. Saxena, T. Chopra, D. Mohanty, Versatile polyketide enzymatic machinery for the biosynthesis of complex mycobacterial lipids, Nat. Prod. Rep. 24 (2) (2007) 267–277, https://doi.org/10.1039/b616817p.
[3] M.J. Nasiri, M. Haeili, M. Ghazi, H. Goudarzi, A. Pormohammad, A.A. Imani Fooladi, M.M. Feizabadi, New insights in to the intrinsic and acquired drug resistance mechanisms in mycobacteria, Front. Microbiol. 25 (8) (2017) 681, https://doi.org/10.3389/fmicb.2017.00681, eCollection 2017.
[4] F. Mougari, L. Guglielmetti, L. Raskine, I. Sermet-Gaudelus, N. Veziris, E. Cambau, Infections caused by Mycobacterium abscessus: epidemiology, diagnostic tools and treatment, Expert Rev. Anti-Infect. Ther. 14 (12) (2016) 1139–1154, https://doi.org/10.1080/14787210.2016.1238304.
[5] R. Nessar, E. Cambau, J.M. Reyrat, A. Murray, B. Gicquel, Mycobacterium abscessus: a new antibiotic nightmare, J. Antimicrob. Chemother. 67 (2012) 810–818, https://doi.org/10.1093/jac/dkr578.
[6] L. Alonso, S.A. Mendanha, M.L. Dorta, A. Alonso, Analysis of the interactions of amphotericin B with the Leishmania plasma membrane using EPR spectroscopy, J. Phys. Chem. B 124 (45) (2020) 10157–10165, https://doi.org/10.1021/acs.jpcb.0c07721.
[7] L. Alonso, S.A. Mendanha, R.S. Gomes, M.L. Dorta, A. Alonso, Comparative EPR spectroscopy analysis of amphotericin B and miltefosine interactions with Leishmania, erythrocyte and macrophage membranes, Eur. J. Pharm. Sci. 163 (2021), 105859, https://doi.org/10.1016/j.ejps.2021.105859.
[8] R.A. Moreira, S.A. Mendanha, K.S. Fernandes, G.G. Matos, L. Alonso, M.L. Dorta, A. Alonso, Miltefosine increases lipid and protein dynamics in Leishmania amazonensis membranes at concentrations similar to those needed for cytotoxicity activity, Antimicrob. Agents Chemother. 58 (2014) 3021–3028, https://doi.org/10.1128/AAC.01332-13.
[9] K.S. Fernandes, P.E. de Souza, M.L. Dorta, A. Alonso, The cytotoxic activity of miltefosine against Leishmania and macrophages is associated with dynamic changes in plasma membrane proteins, Biochim. Biophys. Acta 1859 (1) (2017) 1–9, https://doi.org/10.1016/j.bbamem.2016.10.008.
[10] L. Alonso, É.J.S. Cardoso, R.S. Gomes, S.A. Mendanha, M.L. Dorta, A. Alonso, Antileishmanial and cytotoxic activities of ionic surfactants compared to those of miltefosine, Colloids Surf. B Biointerfaces 183 (2019), 110421, https://doi.org/10.1016/j.colsurfb.2019.110421.
[11] L. Alonso, E.J.S. Cardoso, S.A. Mendanha, A. Alonso, Interactions of miltefosine with erythrocyte membrane proteins compared to those of ionic surfactants, Colloids Surf. B Biointerfaces 180 (2019) 23–30, https://doi.org/10.1016/j.colsurfb.2019.04.040.
[12] H.S. Camargos, R.A. Moreira, S.A. Mendanha, K.S. Fernandes, M.L. Dorta, A. Alonso, Terpenes increase the lipid dynamics in the Leishmania plasma membrane at concentrations similar to their IC50 values, PLoS One 9 (8) (2014), e104429, https://doi.org/10.1371/journal.pone.0104429.
[13] L. Alonso, K.S. Fernandes, S.A. Mendanha, P.J. Gonçalves, R.S. Gomes, M.L. Dorta, A. Alonso, In vitro antileishmanial and cytotoxic activities of nerolidol are associated with changes in plasma membrane dynamics, Biochim. Biophys. Acta Biomembr. 1861 (6) (2019 Jun 1) 1049–1056, https://doi.org/10.1016/j.bbamem.2019.03.006.
[14] T.M. Anderson, M.C. Clay, A.G. Cioffi, K.A. Diaz, G.S. Hisao, M.D. Tuttle, A. J. Nieuwkoop, G. Comellas, N. Maryum, S. Wang, B.E. Uno, E.L. Wildeman, T. Gonen, C.M. Rienstra, M.D. Burke, Amphotericin forms an extramembranous and fungicidal sterol sponge, Nat. Chem. Biol. 10 (5) (2014) 400–406, https://doi.org/10.1038/nchembio.1496.
[15] D.M. Kamiński, Recent progress in the study of the interactions of amphotericin B with cholesterol and ergosterol in lipid environments, Eur. Biophys. J. 43 (2014) 453–467, https://doi.org/10.1007/s00249-014-0983-8.
[16] M. Tayyebi, E. Darchini-Maragheh, P. Layegh, B. Kiafar, V.M. Goyonlo, The effect of oral miltefosine in treatment of antimoniate resistant anthroponotic cutaneous leishmaniasis: an uncontrolled clinical trial, PLoS Negl. Trop. Dis. 15 (3) (2021), e0009241, https://doi.org/10.1371/journal.pntd.0009241.
[17] F. Widmer, L.C. Wright, D. Obando, R. Handke, R. Ganendren, D.H. Ellis, T. C. Sorrell, Hexadecylphosphocholine (miltefosine) has broad-spectrum fungicidal activity and is efficacious in a mouse model of cryptococcosis, Antimicrob. Agents Chemother. 50 (2006) 414–421, https://doi.org/10.1128/AAC.50.2.414-421.2006.
[18] C.C. Spadari, F.W.M.D.S. de Bastiani, L.B. Lopes, K. Ishida, Alginate nanoparticles as non-toxic delivery system for miltefosine in the treatment of candidiasis and cryptococcosis, Int. J. Nanomedicine 14 (2019) 5187–5199, https://doi.org/10.2147/IJN.S205350.
[19] J. Lorenzo-Morales, N.A. Khan, J. Walochnik, An update on Acanthamoeba keratitis: diagnosis, pathogenesis and treatment, Parasite 22 (2015) 10, https://doi.org/10.1051/parasite/2015010.
[20] D. Llull, L. Rivas, E. García, In vitro bactericidal activity of the antiprotozoal drug miltefosine against Streptococcus pneumoniae and other pathogenic streptococci, Antimicrob. Agents Chemother. 51 (2007) 1844–1848, https://doi.org/10.1128/AAC.01428-06.
[21] O. Fleitas Martínez, M.H. Cardoso, S.M. Ribeiro, O.L. Franco, Recent advances in anti-virulence therapeutic strategies with a focus on dismantling bacterial membrane microdomains, toxin neutralization, Quorum-Sensing interference and biofilm inhibition, Front. Cell Infect. Microbiol. 9 (2019 Apr 2) 74, https://doi.org/10.3389/fcimb.2019.00074.
[22] M.M. Eissa, R.M. El-Moslemany, A.A. Ramadan, E.I. Amer, M.Z. El-Azzouni, L. K. El-Khordagui, Miltefosine lipid nanocapsules for single dose oral treatment of Schistosomiasis mansoni: a preclinical study, PLoS One 10 (11) (2015), e0141788, https://doi.org/10.1371/journal.pone.0141788 eCollection 2015.

[23] A.O. Pereira, J.M. Avila, G. Do Carmo, F.S. Siqueira, M.M.A. Campos, D.F. Back, A. F. Morel, I. Dalcol, Chemical composition, antimicrobial and antimycobacterial activities of Aristolochia triangularis Cham. from Brazil, Ind. Crop. Prod. 121 (2018) 461–467, https://doi.org/10.1016/j.indcrop.2018.05.052.
[24] D.F. de Moura, T.A. Rocha, Barros D. de Melo, M.M. da Silva, Santana M. Dos Santos, B.M. Neta, I.M.F. Cavalcanti, R.D. Martins, M.V. da Silva, Evaluation of the antioxidant, antibacterial, and antibiofilm activity of the sesquiterpene nerolidol, Arch. Microbiol. 203 (7) (2021 Sep) 4303–4311, https://doi.org/10.1007/s00203-021-02377-5.
[25] M.J. Park, K.S. Gwak, I. Yang, K.W. Kim, E.B. Jeung, J.W. Chang, I.G. Choi, Effect of citral, eugenol, nerolidol and alpha-terpineol on the ultrastructural changes of Trichophyton mentagrophytes, Fitoterapia 80 (2009) 290–296.
[26] S. Johann, F.B. Oliveira, E.P. Siqueira, P.S. Cisalpino, C.A. Rosa, T.M. Alves, C. L. Zani, B.B. Cota, Activity of compounds isolated from Baccharis dracunculifolia D.C. (Asteraceae) against Paracoccidioide brasiliensis, Med. Mycol. 8 (2012) 843–851.
[27] S. Hoet, C. Stévigny, M.F. Hérent, J. Quetin-Leclercq, Antitrypanosomal compounds from the leaf essential oil of Strychnos spinosa, Planta Med. 5 (2006) 480–482.
[28] D. Arruda, F. D'Alexandri, A. Katzin, S. Uliana, Antileishmanial activity of the terpene nerolidol, Antimicrob. Agents Chemother. 49 (2005) 1679–1687.
[29] A.Y. Saito, A.A. Marin Rodriguez, D.S. Menchaca Vega, R.A.C. Sussmann, E. A. Kimura, A.M. Katzin, Antimalarial activity of the terpene nerolidol, Int. J. Antimicrob. Agents 48 (6) (2016) 641–646.
[30] M. AbouLaila, T. Sivakumar, N. Yokoyama, I. Igarashi, Inhibitory effect of terpene nerolidol on the growth of Babesia parasites, Parasitol. Int. 59 (2) (2010) 278–282.
[31] A.M. Cardoso, A.P. Junqueira-Kipnis, A. Kipnis, In vitro antimicrobial susceptibility of Mycobacterium massiliense recovered from wound samples of patients submitted to arthroscopic and laparoscopic surgeries, Minim. Invasive Surg. 1–4 (2011), https://doi.org/10.1155/2011/724635.
[32] D.E. Griffith, T. Aksamit, B.A. Brown-Elliott, A. Catanzaro, C. Daley, F. Gordin, et al., An official ATS/IDSA statement: diagnosis, treatment, and prevention of nontuberculous mycobacterial diseases, Am. J. Respir. Crit. Care Med. 175 (2007) 367–416, pmid:17277290.
[33] D.J. Schneider, J.H. Freed, Biological magnetic resonance, in: L.J. Berliner, J. Reuben (Eds.), Spin Labeling: Theory and Application, Plenum Press, New York, 1989, pp. 1–76.
[34] D.E. Budil, S. Lee, S. Saxena, J.H. Freed, Nonlinear-least-squares analysis of slow-motion EPR spectra in one and two dimensions using a modified Levenberg–Marquardt algorithm, J. Mag. Reson. Ser A 120 (1986) 155–189, https://doi.org/10.1006/jmra.1996.0113.
[35] P.C. Jost, O.H. Griffith, R.A. Capaldi, G. Vanderkooi, Evidence for boundary lipid in membranes, Proc. Natl. Acad. Sci. U. S. A. 70 (1973) 480–484, https://doi.org/10.1073/pnas.70.2.480.
[36] D. Marsh, Electron spin resonance in membrane research: protein-lipid interactions from challenging beginnings to state of the art, Eur. Biophys. J. 39 (2010) 513–525, https://doi.org/10.1007/s00249-009-0512-3.
[37] J.L. Anjos, S. Neto Dde, A. Alonso, Effects of 1,8-cineole on the dynamics of lipids and proteins of stratum corneum, Int. J. Pharm. 345 (1–2) (2007) 81–87, https://doi.org/10.1016/j.ijpharm.2007.05.041.
[38] J.L. dos Anjos, Neto D. de Sousa, A. Alonso, Effects of ethanol/l-menthol on the dynamics and partitioning of spin-labeled lipids in the stratum corneum, Eur. J. Pharm. Biopharm. 67 (2) (2007) 406–412, https://doi.org/10.1016/j.ejpb.2007.02.004.
[39] R.A. Neal, S.L. Croft, An in-vitro system for determining the activity of compounds against the intracellular amastigote form of Leishmania donovani, J. Antimicrob. Chemother. 14 (5) (1984) 463–475, https://doi.org/10.1093/jac/14.5.463.
[40] A.R. Garcia, A.C.F. Amaral, M.M.B. Azevedo, S. Corte-Real, R.C. Lopes, C. S. Alviano, A.S. Pinheiro, A.B. Vermelho, I.A. Rodrigues, Cytotoxicity and anti-Leishmania amazonensis activity of Citrus sinensis leaf extracts, Pharm. Biol. 55 (1) (2017) 1780–1786, https://doi.org/10.1080/13880209.2017.1325380.
[41] S.L. Croft, G.H. Coombs, Leishmaniasis–current chemotherapy and recent advances in the search for novel drugs, Trends Parasitol. 19 (11) (2003) 502–508, https://doi.org/10.1016/j.pt.2003.09.008.
[42] L. Alonso, S.A. Mendanha, C.A. Marquezin, M. Berardi, A.S. Ito, A.U. Acuña, A. Alonso, Interaction of miltefosine with intercellular membranes of stratum corneum and biomimetic lipid vesicles, Int. J. Pharm. 434 (1–2) (2012) 391–398, https://doi.org/10.1016/j.ijpharm.2012.06.006.
[43] R.A. Moreira, S.A. Mendanha, D. Hansen, A. Alonso, Interaction of miltefosine with the lipid and protein components of the erythrocyte membrane, J. Pharm. Sci. 102 (5) (2013) 1661–1669, https://doi.org/10.1002/jps.23496.
[44] S.A. Mendanha, S.S. Moura, J.L. Anjos, M.C. Valadares, A. Alonso, Toxicity of terpenes on fibroblast cells compared to their hemolytic potential and increase in erythrocyte membrane fluidity, Toxicol. in Vitro 27 (1) (2013) 323–329, https://doi.org/10.1016/j.tiv.2012.08.022.
[45] N.S. Thomas, R. Panchagnula, Transdermal delivery of zidovudine: effect of vehicles on permeation across rat skin and their mechanism of action, Eur. J. Pharm. Sci. 18 (2003) 71–79.
[46] S.A. Mendanha, A. Alonso, Effects of terpenes on fluidity and lipid extraction in phospholipid membranes, Biophys. Chem. 198 (2015) 45–54, https://doi.org/10.1016/j.bpc.2015.02.001.